

## Research Article

# Molding Properties of Inconel 718 Feedstocks Used in Low-Pressure Powder Injection Molding

**Fouad Fareh,<sup>1</sup> Vincent Demers,<sup>1</sup> Nicole R. Demarquette,<sup>1</sup>  
Sylvain Turenne,<sup>2</sup> and Orlando Scalzo<sup>3</sup>**

<sup>1</sup>*École de Technologie Supérieure, 1100 Notre-Dame West, Montréal, QC, Canada H3C 1K3*

<sup>2</sup>*Polytechnique Montréal, 2500 Chemin de Polytechnique, Montréal, QC, Canada H3T 1J4*

<sup>3</sup>*Pratt & Whitney Canada, 1000 boulevard Marie-Victorin, Longueuil, QC, Canada J4G 1A1*

Correspondence should be addressed to Vincent Demers; [vincent.demers@etsmtl.ca](mailto:vincent.demers@etsmtl.ca)

Received 23 May 2016; Accepted 20 June 2016

Academic Editor: Charles C. Sorrell

Copyright © 2016 Fouad Fareh et al. This is an open access article distributed under the Creative Commons Attribution License, which permits unrestricted use, distribution, and reproduction in any medium, provided the original work is properly cited.

The impact of binders and temperature on the rheological properties of feedstocks used in low-pressure powder injection molding was investigated. Experiments were conducted on different feedstock formulations obtained by mixing Inconel 718 powder with wax-based binder systems. The shear rate sensitivity index and the activation energy were used to study the degree of dependence of shear rate and temperature on the viscosity of the feedstocks. The injection performance of feedstocks was then evaluated using an analytical moldability model. The results indicated that the viscosity profiles of feedstocks depend significantly on the binder constituents, and the secondary binder constituents play an important role in the rheological behavior (pseudoplastic or near-Newtonian) exhibited by the feedstock formulations. Viscosity values as low as 0.06 to 2.9 Pa·s were measured at high shear rates and high temperatures. The results indicate that a feedstock containing a surfactant agent exhibits the best moldability characteristics.

## 1. Introduction

Low-pressure powder injection molding (LPIM) is a cost-effective emerging technology for producing small and complex parts, either in high or in low production volumes. This rapid manufacturing process consists in mixing metallic or ceramic powder with molten polymeric binder to obtain a feedstock which is injected into a mold cavity to produce parts with complex shape. During debinding and sintering treatments, the binder is completely removed to obtain a near-net shape dense metallic component [1]. Recent progress in feedstock formulations [2–4] has generated new opportunities for the injection of low-viscosity (<4 Pa·s) molten powder-binder mixtures (<100°C) into a mold cavity using an injection pressure generally lower than 700 kPa [5, 6]. Initially used in ceramics forming [7–9], the LPIM technology has quickly become attractive for the development of high value-added metallic parts in the aerospace industry [10].

Inconel 718 is an age-hardenable nickel-based superalloy extensively used in the aerospace field and in many other applications requiring the combination of high tensile strength, fatigue strength, creep resistance, and oxidation resistance at elevated temperatures. However, shaping difficulties, such as poor machinability and formability, limit their applications for complex shaped parts. It was reported in [11, 12] that Inconel 718 powder can be consolidated in the range of 92–97% of the theoretical density using the conventional metal injection molding method. However, low-pressure injection molding of Inconel 718 parts has received very little attention in the literature.

Feedstock viscosity is one of the most important parameters influencing the success of the molding stage. The main variables influencing the viscosity of powder-binder mixtures are shear rate, temperature, solid loading, powder characteristics (shape and size), and binder composition [6, 13–15]. It has also been reported that the moldability index model developed for plastic injection molding [16], and more

recently exploited in conventional metal injection molding [17–19] or in LPIM of metal matrix composites part [20, 21], could be used to predict the flow behavior of the feedstocks during injection. Recently, the rheological properties of LPIM stainless steel feedstocks were investigated using the flow behavior index and activation energy [22]. However, the molding potential for these metallic feedstocks was not evaluated using the moldability index model. For LPIM Inconel 718 feedstocks, the characterization of the rheological behavior is still in infancy [15], and the moldability index model has never been used to calculate the molding potential of such feedstocks. Hence, this work aims to investigate the molding properties of Inconel 718 superalloy feedstocks used in low-pressure powder injection molding.

## 2. Experimental Procedures

**2.1. Materials.** Gas-atomized Inconel 718 superalloy powder (Sandvik Osprey, Neath, UK), with a typical spherical shape and an average particle size of  $12\ \mu\text{m}$ , was used (Figure 1). The melting temperatures of the binders used in the present study are listed in Table 1. Due to their extensive use in LPIM, paraffin wax (PW) and beeswax (BW) with melting points ranging from 55 to  $65^\circ\text{C}$  were compared. Stearic acid (SA) and ethylene vinyl acetate (EVA) were used as surfactant and thickening agents, respectively. Surfactant agent acts as a bridge between the metallic powder and the other constituents to enhance the homogeneity of the feedstock as well as the mixing properties. Thickening agent is generally used to increase the viscosity of the mixture in order to prevent powder-binder separation. Stearic acid, oleic acid, ethylene vinyl acetate, and low-density polyethylene are extensively used as the secondary constituents in LPIM feedstocks [5, 23–26]. From an injection process perspective, German [23] proposes that a good binder should have good adhesion with powder and low viscosity ( $<10\ \text{Pa}\cdot\text{s}$ ) at the molding temperature. These polymer constituents were mixed with the metallic powder to form homogeneous feedstocks according to the powder-binder formulations given in Table 1. In this study, simple feedstocks (single- or dual-binder constituent) were used to better understand the impact of each binder constituent on the molding properties of feedstocks, which is a necessary basic step for future development of more complex LPIM multibinder feedstocks. Varying typically from 55 to 70 vol.%, the solid loading of feedstocks was kept constant at 60 vol.% in order to ensure the wettability of metallic powder with single-binder constituent (e.g., feedstocks 40PW and 40BW) and obtain homogeneous powder-binder mixtures. The volume fractions of powder presented in this study are the values determined at room temperature, and the feedstock identification is referenced by their polymer volume fraction. For example, the feedstock 35PW-5SA is a mixture containing 60 vol.% of powder with 35 vol.% of paraffin wax and 5 vol.% of stearic acid.

**2.2. Measurement.** The viscosity of the feedstocks was measured by an Anton Paar MCR 501 rotational rheometer using the concentric-cylinder C-PTD200, with a Peltier temperature controlled measuring system. The samples were

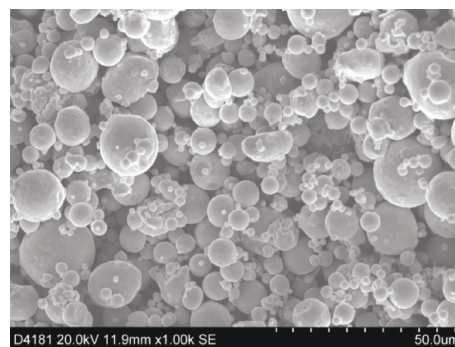


FIGURE 1: SEM micrograph of Inconel 718 powder.

poured into the barrel, presheared at  $50\ \text{s}^{-1}$  (to reach thermal equilibrium), and then tested at shear rates ranging from 1 to  $3000\ \text{s}^{-1}$  for temperatures ranging from 70 to  $100^\circ\text{C}$ . The melting temperature of binders was measured by a TA Instrument Q2000 differential scanning calorimeter (DSC). The DSC tests were performed in a temperature range of 10 to  $100^\circ\text{C}$ , using a heating rate of  $10^\circ\text{C}\cdot\text{min}^{-1}$  and a nitrogen gas flow rate of  $50\ \text{mL}\cdot\text{min}^{-1}$ . Specimens with a mass ranging from 8 to 12 mg were encapsulated in standard aluminum hermetic pans. The DSC graphs were recorded from the second heating cycle. In the case where the thermal profiles exhibit more than one peak, the melting point of binder was measured using the last characteristic peak as indicated by a black arrow on DSC graphs while the white arrows show the other characteristic peaks (see Figure 2). The melting point of binder was used to determine the minimum temperature for rheological testing. From a practical perspective, the melting point of binder provides the minimum injection temperature for a given powder-binder mixture. Thermogravimetric analysis (TGA) was used to measure the decomposition temperatures of feedstocks. The TGA tests were performed using a Perkin Elmer Diamond TG/DTA. Specimens were placed in standard platinum pans and heated from 20 to  $800^\circ\text{C}$  (heating rate of  $20^\circ\text{C}/\text{min}$ ) under high purity nitrogen purge gas (flow rate of  $60\ \text{mL}/\text{min}$ ). TGA was used to determine the maximal temperature for rheological testing. From a practical perspective, the start and finish temperatures for degradation of binder are generally used to evaluate the debinding temperatures of molded parts.

## 3. Results and Discussion

Figure 2 presents the DSC results obtained for the four feedstocks of this study. In addition, thermograms for stearic acid and ethylene vinyl acetate are presented. Note that the rheological testing was not performed with the feedstocks 40SA and 40EVA (i.e., feedstocks containing only stearic acid or only ethylene vinyl acetate) but their DSC thermograms were obtained to evaluate the solubility or the interaction with the paraffin wax. The melting point of the feedstocks was reported in Table 1. The minimum temperature for rheological testing was selected at  $70^\circ\text{C}$  because the highest melting point obtained with the feedstock 35PW-5EVA is

TABLE 1: Nominal volume fraction and melting temperatures of the binders used for the feedstocks.

Feedstock identification	Vol.% [%]					Melting point [°C]	Temperature of degradation [°C]	
	Metallic powder	Paraffin wax (PW)	Beeswax (BW)	Stearic acid (SA)	Ethylene vinyl acetate (EVA)		Start	Finish
40PW	60	40	—	—	—	55	150	300
40BW	60	—	40	—	—	65	225	500
35PW-5SA	60	35	—	5	—	54	150	300
35PW-5EVA	60	35	—	—	5	66	175	500

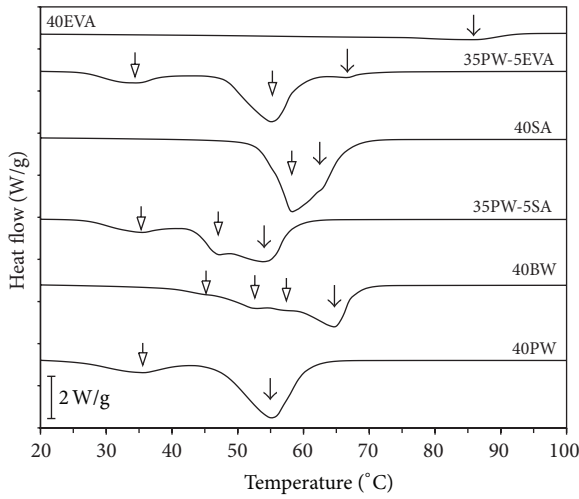


FIGURE 2: DSC thermogram of binders.

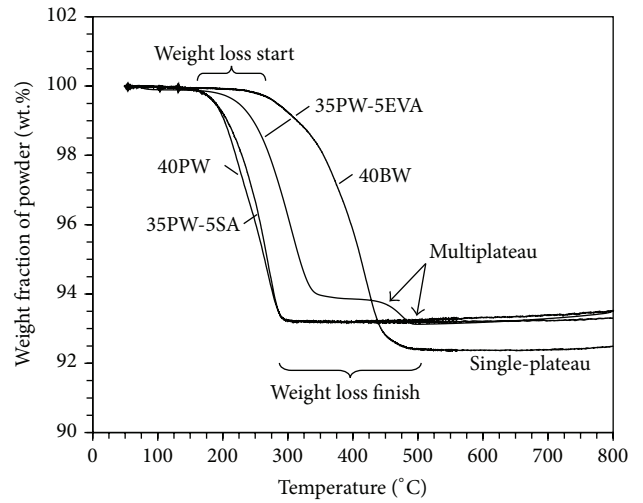


FIGURE 3: TGA profiles of feedstocks.

66°C. Figure 2 shows that the paraffin wax has a certain degree of solubility with stearic acid and ethylene vinyl acetate. Compared to the feedstock 40PW, an addition of 5 vol.% of stearic acid in the paraffin wax changes the thermal profile but not really the melting point of the feedstock 35PW-5SA. Indeed, the feedstocks containing only paraffin wax (40PW) and only stearic acid (40SA) have two different melting points, but the molten state of the feedstock 35PW-5SA is reached at the same temperature compared to that of the feedstock 40PW. On the other hand, the melting point of the paraffin-wax-EVA mixture (35PW-5EVA) is significantly lower than that of pure EVA feedstock. The combination of paraffin wax with 5 vol.% of EVA results in DSC graphs characterized by the two distinct peaks of the paraffin wax and a third peak at 66°C. In that respect, the SA and EVA can be added in paraffin wax to tailor the rheological properties of feedstocks in order to decrease viscosity and to prevent powder-binder separation without inducing a significant increase in melting temperature of the feedstock.

Figure 3 presents the TGA profiles obtained for different wax-based feedstocks. The remaining mass after binder burnout was divided by the total mass before binder burnout to calculate the weight fraction of powder (wt.%) in feedstock. As illustrated in Figure 3, a single-binder and a multibinder

feedstock produce, respectively, a single-plateau and a multi-plateau TGA curve. Weight loss starts between 150 and 225°C. The binder is completely burned over a temperature range of about 300–500°C depending on the feedstock formulation. Temperature of degradation of each constituent is reported in Table 1. Weight fraction of powder is generally affected by solid loading of the feedstock [27]. In this study, the solid loading was kept constant and thus the higher weight fraction of powder obtained with 40BW is explained by a higher density of this constituent. The maximum temperature for rheological testing was defined at 100°C which is below the start temperature of the degradation of all binders.

Figure 4 presents the viscosity profiles obtained at different temperatures for different wax-based feedstocks. The rheological behavior of LPIM feedstocks depends significantly on the binder constituents. The viscosity of feedstocks containing only paraffin wax and only beeswax, as well as that formulated with paraffin wax and stearic acid, decreases with shear rate, which corresponds to the pseudoplastic behavior generally required for LPIM feedstock (Figures 4(a), 4(b), and 4(c)). This pseudoplastic behavior is explained by a particle or binder molecule orientation and ordering with flow. The deagglomeration of the particles and the formation of the preferential flow layers promote a decrease in viscosity

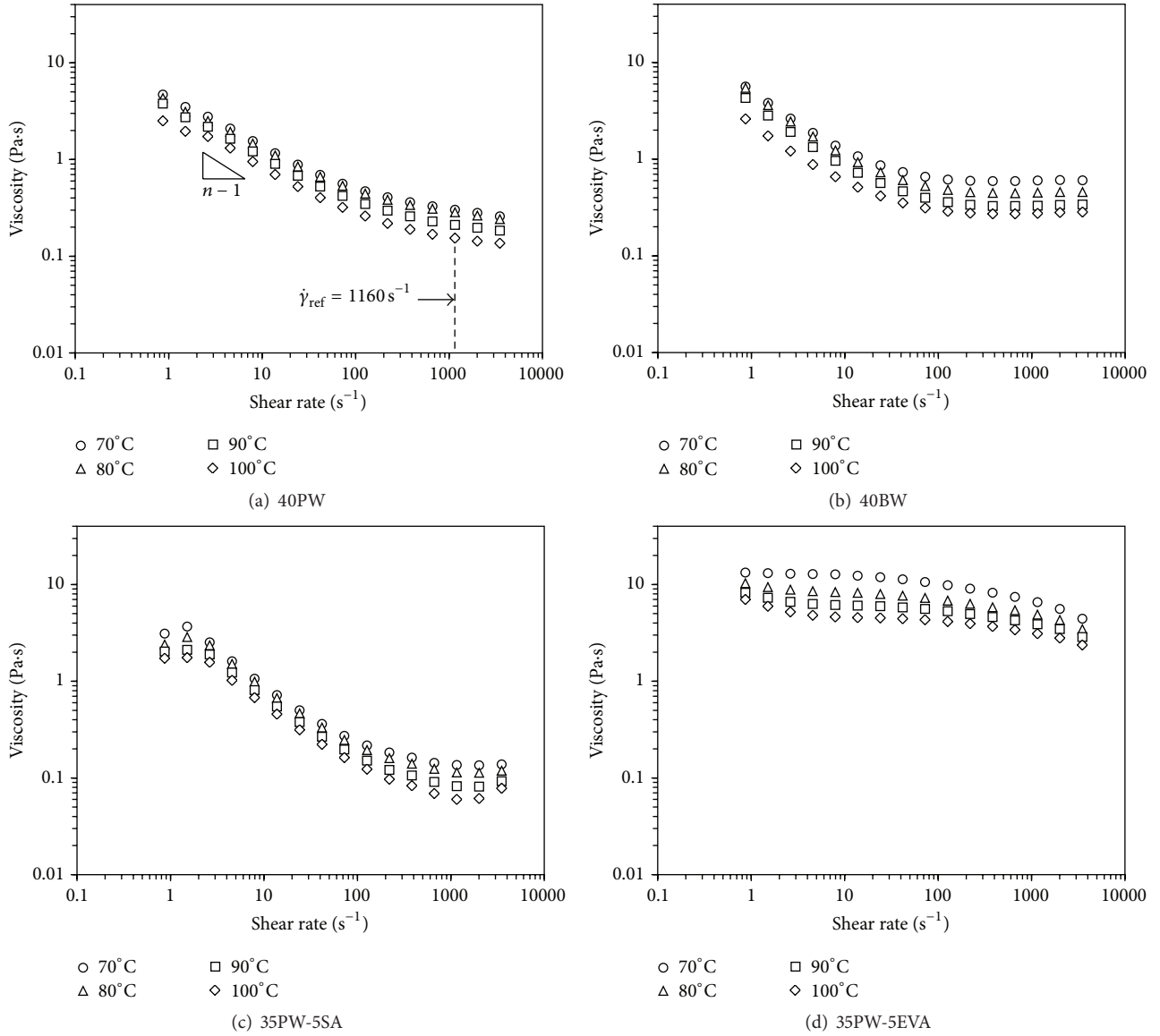


FIGURE 4: Viscosity profiles of feedstocks at different temperatures.

with an increase in the shear rate. Although their viscosity profiles are slightly different, a similar minimum viscosity value of around 0.1–0.3 Pa.s was obtained for these three feedstocks (40PW, 40BW, and 35PW-5SA). This very low viscosity is suitable for low-pressure injection. The feedstock 35PW-5EVA is characterized by a near-Newtonian behavior, with relatively high viscosity values across the entire shear rate range (Figure 4(d)). The feedstock 35PW-5EVA produces relatively high viscosity values (about 10 times higher than the three previous feedstocks) and an absence of pseudoplastic behavior, which are generally not the required flow properties for an LPIM process. The viscosity values at a reference shear rate ( $\dot{\gamma}_{\text{ref}} = 1160 \text{ s}^{-1}$ ) were extracted from Figure 4 and summarized in Table 2 for each testing condition. This reference shear rate corresponds to a target value at which the viscosity

is low and constant during the injection for many feedstocks.

The flow characteristics of feedstocks can be described by the power-law (see (1)) model widely reported in the literature [17]:

$$\eta = K\dot{\gamma}^{n-1}, \quad (1)$$

where  $\eta$  is the feedstock viscosity,  $\dot{\gamma}$  the shear rate,  $K$  is a constant, and  $n$  is the shear rate sensitivity index. The values of  $n$  were calculated from the slope  $n-1$  of the viscosity profiles presented in Figure 4 and summarized in Table 2, for each testing condition. This shear rate sensitivity index indicates the degree of dependence of the shear rate on the feedstock viscosity during the injection. Generally, the value of  $n$  should be as small as possible to maximize the viscosity changes

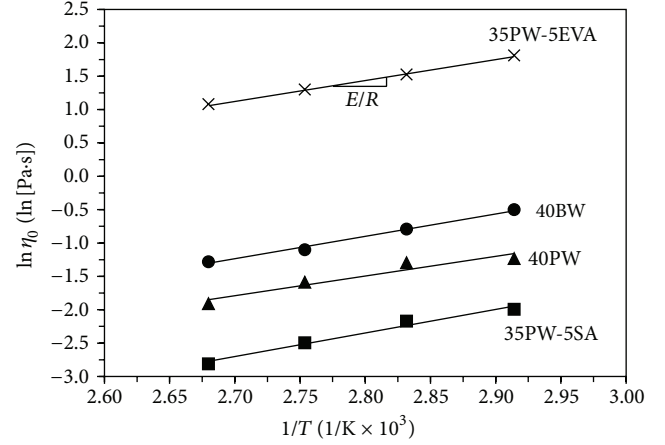
TABLE 2: Rheological parameters of feedstocks.

Feedstock	Temperature (°C)	$\eta_0$ (Pa·s)	$n$	$E$ (kJ/mol)
40PW	70	0.29	0.59	24.5
	80	0.27	0.60	24.5
	90	0.20	0.57	24.5
	100	0.15	0.54	24.5
40BW	70	0.61	0.56	28.3
	80	0.45	0.52	28.3
	90	0.33	0.51	28.3
	100	0.28	0.57	28.3
35PW-5SA	70	0.14	0.41	29.5
	80	0.11	0.39	29.5
	90	0.08	0.37	29.5
	100	0.06	0.36	29.5
35PW-5EVA	70	6.11	0.92	25.8
	80	4.59	0.91	25.8
	90	3.67	0.91	25.8
	100	2.94	0.90	25.8

during and after the mold filling. Before or after injection, the viscosity of feedstock should be as high as possible to prevent powder-binder separation in the injection channel of the injection press as well as within the injected part. However, the viscosity during the injection operation must be as low as possible to increase the moldability potential of the feedstock, or in other words to increase the complexity of the part that could be molded. In that respect, the combination of the value of  $n$  with the maximum viscosity (usually obtained at low shear rate) or the minimum viscosity (usually obtained at high shear rate) could be more appropriate to evaluate the rheological behavior of different feedstocks. As shown in Figure 4, the viscosity of a feedstock decreases with an increase in temperature as expected in the well-known Arrhenius equation:

$$\eta = \eta_{T0} \exp\left(\frac{E}{RT}\right), \quad (2)$$

where  $\eta_{T0}$  is the viscosity at a reference temperature,  $E$  the activation energy,  $R$  the gas constant, and  $T$  the temperature. The values for the natural logarithm of the viscosity  $\eta_0$  measured at the reference shear rate (see Table 2) were plotted against the inverse of the temperature in Figure 5. According to (2), the slope of the  $\ln(\eta_0) - 1/T$  graph is  $E/R$ , from which the values of  $E$  were calculated and summarized in Table 2 for each feedstock. This activation energy quantifies the effect of temperature on the viscosity, which should be as small as possible to minimize significant changes of feedstock viscosity between the hot and cold zones in the injection press or in the mold.

FIGURE 5: Viscosity of feedstocks as a function of temperature (at  $\dot{\gamma}_{\text{ref}} = 1160 \text{ s}^{-1}$ ).

The molding capability of feedstocks during injection can be studied using the Weir model (see (3)) initially developed for the injection molding of plastic [16]:

$$\alpha_{\text{STV}} = \frac{10^8 |n - 1|}{\eta_0 E/R}, \quad (3)$$

where  $\alpha_{\text{STV}}$  is the moldability index while other rheological parameters are as described above. This simple but original model describes the rheological behavior of feedstocks by combining several rheological parameters. From a practical perspective, the moldability is the ability of the feedstock to be injected into the mold cavity with few defects (such as incomplete mold filling, cracks, and porosities). The moldability index was recently introduced in PIM to evaluate the properties of feedstocks during mold filling. From a molding perspective, the best feedstock candidate corresponds to the highest value of the moldability index (i.e., lowest value of  $\eta_0$ ,  $n$ , and  $E$ , concurrently).

Figure 6 shows the moldability index of feedstocks at different temperatures, which were calculated from the rheological parameters summarized in Table 2. As expected, the moldability index increases as the temperature of the feedstocks increases. In this study, the feedstock 35PW-5SA exhibits the best moldability characteristics. The enhancement of the rheological properties of this feedstock is attributable to the surfactant effect of the stearic acid between the powder and the main wax-based binder constituent. In this respect, it is interesting to note that an addition of 5 vol.% of stearic acid in a feedstock at 70°C generates a similar moldability index to a feedstock formulation at 100°C containing only paraffin wax. For the feedstock 35PW-5SA, the significant variation of the moldability index values according to the temperature can be attributable to the significant change in the values of viscosity  $\eta_0$  obtained between 70 and 100°C. In other words, the molding properties of feedstock containing paraffin wax and stearic acid are more affected by the temperature than that containing only paraffin wax. The ethylene vinyl acetate is generally used as a thickening agent. Poor moldability index results (below 1000) obtained for the



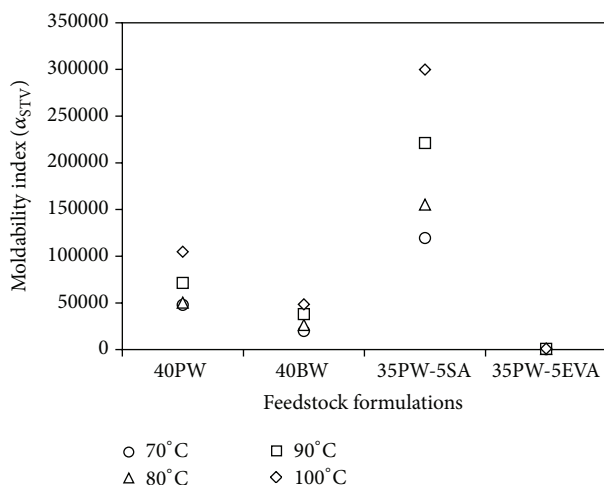


FIGURE 6: Moldability index ( $\alpha_{STV}$ ) of feedstocks at different temperatures (for  $\dot{\gamma}_{ref} = 1160 \text{ s}^{-1}$ ).

feedstock 35PW-5EVA suggest that this simple mixture is not suitable for the LPIM process and should be potentially used with other combinations of wax-based binders in order to tailor the rheological properties of feedstocks. Finally, the molding characteristics of the feedstock containing only paraffin wax (40PW) are slightly more pronounced than those of the mixture containing only beeswax (40BW). However, the moldability index of feedstock 40BW is less affected by the temperature than that of the feedstock 40PW. Therefore, these two wax constituents are good candidates for development of low-viscosity Inconel 718 feedstocks, and their moldability potential within multibinders mixtures will be demonstrated in future work.

In this study, the moldability index was calculated for different feedstocks and temperatures. However, the solid loading of powder has an impact on the moldability of feedstock. Ghanbari et al. [21] have demonstrated that the moldability index of LPIM metal matrix composite feedstock can be doubled with a change in four percentage point of solid loading. On the other hand, Hidalgo et al. [18] have determined the optimal solid loading generating the highest value of moldability index for LPIM ceramic feedstock. Therefore, a decrease in moldability potential of Inconel 718 feedstocks is expected with an increase in solid loading. The impact of the solid loading on the moldability index for Inconel 718 feedstocks will be quantified in future work.

Finally, the degradation temperature was also used to define the best candidate feedstocks. From a practical perspective, the finish temperature for degradation of binder is generally used to evaluate the debinding temperatures plateau at which the binder is extracted and then burned. In general, this temperature should be as low as possible to limit the oxidation of the debound parts during furnace debinding. Considering the values of the degradation temperature reported in Table 1 and the moldability index values summarized in Figure 6, the feedstock 35PW-5SA generates a low degradation temperature combined with the highest moldability potential. Therefore, mixture containing paraffin

wax and stearic acid could be used for future development of Inconel 718 feedstocks.

#### 4. Conclusion

The rheological behavior low-pressure injection molding feedstocks were investigated. Simple feedstocks (single- or dual-binder constituent) were used to better understand the impact of each binder constituent on the molding properties of feedstocks and to define the basis for future development of more complex multibinder superalloys feedstocks. Rotational rheometer was used to measure the viscosity profiles on different Inconel 718 superalloy feedstocks. Differential scanning calorimetry and thermogravimetric analysis were used to measure the melting point and degradation temperature of binders in order to define the temperature limits of the rheological testing. The fundamental rheological parameters, such as the shear rate sensitivity index ( $n$ ) and the activation energy ( $E$ ), were calculated from the viscosity profiles, and the moldability index ( $\alpha_{STV}$ ) was evaluated for each feedstock.

The results obtained at different temperatures confirmed that paraffin wax (PW), beeswax (BW), and stearic acid (SA) can be used to decrease the viscosity of the feedstock while the purpose of ethylene vinyl acetate (EVA) is to increase the viscosity of the feedstock. The feedstocks 40PW, 40BW, and 35PW-5SA showed pseudoplastic behavior with values of shear rate sensitivity index ranging from 0.36 to 0.60, while the feedstock 35PW-5EVA is characterized by a near-Newtonian behavior with relatively high values of the viscosity in the entire shear rate range ( $n \approx 0.91$ ). The feedstock containing paraffin wax and stearic acid (35PW-5SA) has exhibited the lower viscosity, the lower shear rate sensitivity index, the higher activation energy, and therefore the higher moldability index. In addition, the feedstock 35PW-5SA generates a low degradation temperature which is suitable to prevent the oxidation during furnace debinding. In the absence of an injection problem, such as feedstock jetting, significant residual stresses, or powder segregation, the best candidate feedstocks are the mixtures containing paraffin wax and stearic acid.

#### Competing Interests

The authors declare that they have no competing interests.

#### Acknowledgments

This work was carried out with the financial support of the Natural Science and Engineering Research Council (NSERC) of Canada (under Grant no. 183917-04). The authors wish to thank Pratt & Whitney Canada and the Polytechnique Montréal Department of Chemical Engineering for the use of their laboratories and characterization equipment.

#### References

- [1] D. Heaney, *Handbook of Metal Injection Molding*, Woodhead, Cambridge, UK, 1st edition, 2012.
- [2] N. Schlechtriemen, R. Knitter, J. Haußelt, and J. R. Binder, "Impact of powder morphology on quality of low-pressure

- injection moulded reaction-bonded net shape oxide ceramics," *Journal of the European Ceramic Society*, vol. 33, no. 4, pp. 709–715, 2013.
- [3] R. A. Ikegami and B. D. M. Purquerio, "Low pressure injection moulding of stainless steel powder," *Key Engineering Materials*, vol. 189–191, pp. 467–472, 2001.
  - [4] R. Waesche, C. Paulick, G. Steinborn, V. Richter, and M. Werner, "Joining of ceramic components in the green state via LPIM," *Advanced Materials Research*, vol. 29–30, pp. 207–210, 2007.
  - [5] L. Gorjan, A. Dakskobler, and T. Kosmač, "Partial wick-debinding of low-pressure powder injection-moulded ceramic parts," *Journal of the European Ceramic Society*, vol. 30, no. 15, pp. 3013–3021, 2010.
  - [6] J. Hidalgo, C. Abajo, A. Jiménez-Morales, and J. M. Torralba, "Effect of a binder system on the low-pressure powder injection moulding of water-soluble zircon feedstocks," *Journal of the European Ceramic Society*, vol. 33, no. 15–16, pp. 3185–3194, 2013.
  - [7] J. E. Zorzi, C. A. Perottoni, and J. A. H. Da Jornada, "Wax-based binder for low-pressure injection molding and the robust production of ceramic parts," *Industrial Ceramics*, vol. 23, no. 1, pp. 47–49, 2003.
  - [8] R. E. F. Q. Nogueira, A. C. Bezerra, F. C. Dos Santos, M. R. De Sousa, and W. Acchar, "Low-pressure injection molding of alumina ceramics using a carnauba wax binder: preliminary results," *Key Engineering Materials*, vol. 189–191, pp. 67–72, 2001.
  - [9] N. Schlechtriemen, J. R. Binder, C. Hane, M. Müller, H.-J. Ritzhaupt-Kleissl, and J. Hausselt, "Manufacturing of net-shape reaction-bonded ceramic microparts by low-pressure injection molding," *Advanced Engineering Materials*, vol. 11, no. 5, pp. 339–345, 2009.
  - [10] B. Julien and M. Després, "Metal injection moulding: a near net shape fabrication method for the manufacture of turbine engine component," in *Cost Effective Manufacture via Net Shape Processing*, pp. 8.1–8.16, Research and Technology Organisation (NATO), Amsterdam, The Netherlands, 2006.
  - [11] Ö. Özgün, H. O. Gulsoy, R. Yilmaz, and F. Findik, "Microstructural and mechanical characterization of injection molded 718 superalloy powders," *Journal of Alloys and Compounds*, vol. 576, pp. 140–153, 2013.
  - [12] R. Ibrahim, M. Azmiruddin, M. Jabir, N. Johari, M. Muhamad, and A. R. A. Talib, "Injection molding of inconel 718 parts for aerospace application using novel binder system based on palm oil derivatives," *International Journal of Mechanical, Aerospace, Industrial, Mechatronic and Manufacturing Engineering*, vol. 6, no. 10, pp. 2112–2116, 2012.
  - [13] M. R. Harun, N. Muhamad, A. B. Sulong, N. H. M. Nor, and M. H. I. Ibrahim, "Rheological investigation of ZK60 magnesium alloy feedstock for metal injection moulding using palm stearin based binder system," *Applied Mechanics and Materials*, vol. 44–47, pp. 4126–4130, 2011.
  - [14] N. H. M. Nor, M. H. Ismail, N. A. Abu Kasim, N. Muhamad, and M. A. Taib, "Characterization and rheological studies on ready-made feedstock of stainless steel 316L in metal injection molding (MIM) process," *Applied Mechanics and Materials*, vol. 465–466, pp. 709–714, 2014.
  - [15] V. Demers, S. Turenne, and O. Scalzo, "Impact of binders on viscosity of low-pressure powder injection molded Inconel 718 superalloy," *Journal of Materials Science*, vol. 50, no. 7, pp. 2893–2902, 2015.
  - [16] F. E. Weir, "Moldability of plastics based on melt rheology. Part 1—theoretical development," *Polymer Engineering & Science*, vol. 3, no. 1, pp. 32–36, 1963.
  - [17] S.-J. Park, Y. Wu, D. F. Heaney, X. Zou, G. Gai, and R. M. German, "Rheological and thermal debinding behaviors in titanium powder injection molding," *Metallurgical and Materials Transactions A: Physical Metallurgy and Materials Science*, vol. 40, no. 1, pp. 215–222, 2009.
  - [18] J. Hidalgo, A. Jiménez-Morales, and J. M. Torralba, "Torque rheology of zircon feedstocks for powder injection moulding," *Journal of the European Ceramic Society*, vol. 32, no. 16, pp. 4063–4072, 2012.
  - [19] M. H. I. Ibrahim, N. Muhamad, and A. B. Sulong, "Rheological investigation of water atomised stainless steel powder for micro metal injection molding," *International Journal of Mechanical and Materials Engineering*, vol. 4, no. 1, pp. 1–8, 2009.
  - [20] M. Khakbiz, A. Simchi, and R. Bagheri, "Investigation of rheological behaviour of 316L stainless steel-3 wt-%TiC powder injection moulding feedstock," *Powder Metallurgy*, vol. 48, no. 2, pp. 144–150, 2005.
  - [21] A. Ghanbari, M. Alizadeh, E. Ghasemi, R. Y. Rad, and S. Ghaffari, "Preparation of optimal feedstock for low-pressure injection molding of Al/SiC nanocomposite," *Science and Engineering of Composite Materials*, vol. 22, no. 5, pp. 549–554, 2015.
  - [22] M. Aslam, F. Ahmad, P. S. M. B. M. Yusoff et al., "Investigation of rheological behavior of low pressure injection molded stainless steel feedstocks," *Advances in Materials Science and Engineering*, vol. 2016, Article ID 5347150, 9 pages, 2016.
  - [23] R. M. German, *Powder Metallurgy Science*, Metal Powder Industries Federation Princeton, New Jersey, NJ, USA, 2nd edition, 1994.
  - [24] M. Rei, E. C. Milke, R. M. Gomes, L. Schaeffer, and J. P. Souza, "Low-pressure injection molding processing of a 316-L stainless steel feedstock," *Materials Letters*, vol. 52, no. 4–5, pp. 360–365, 2002.
  - [25] Y.-M. Li, X.-Q. Liu, F.-H. Luo, and J.-L. Yue, "Effects of surfactant on properties of MIM feedstock," *Transactions of Nonferrous Metals Society of China*, vol. 17, no. 1, pp. 1–8, 2007.
  - [26] A. Dakskobler and T. Kosmač, "Rheological properties of remelted paraffin-wax suspensions used for LPIM," *Journal of the European Ceramic Society*, vol. 29, no. 10, pp. 1831–1836, 2009.
  - [27] V. Demers, S. Turenne, and O. Scalzo, "Segregation measurement of powder injection molding feedstock using thermogravimetric analysis, pycnometer density and differential scanning calorimetry techniques," *Advanced Powder Technology*, vol. 26, no. 3, pp. 997–1004, 2015.